

# Hostos Journal of Student Research

A Publication of the Natural Sciences Department, Hostos Community College, CUNY

2013

Volume 4, Issue 1

In this issue:	Pages
Table of Content/Letter from the Editors .....	1
Roller Coaster Marbles: Converting Potential Energy to Kinetic Energy..... Ricky Bhola, Ibrahim Alassani, Emilie Bouda, Jaime Luján and Yoel Rodríguez	2
Cloning and Expression of <i>CDC13</i> gene from <i>Candida parapsilosis</i> ..... Rosario Ana	7
<i>CpCdc13</i> Interaction with <i>Candida parapsilosis</i> and <i>Candida lusitania</i> Telomeres..... Perez Eliana	14
Submission Guide.....	20
Internship opportunities.....	21

Dear Student,

In this issue of the journal we offer you three research articles authored by your fellow students of the Hostos Community College.

We hope that you will enjoy all of these articles, and follow these authors in sharing your educational experience with Hostos community on the pages of the Hostos Journal of Students Research.

Editorial Board

# Roller Coaster Marbles: Converting Potential Energy to Kinetic Energy.

Ricky Bholá, Ibrahim Alassani, and Emilie Bouda  
Natural Sciences Department, Hostos Community College, Bronx, New York

The 18th century scientific revolution exposed many new ideas and concepts of the natural world. Among these are the conservation laws governing energy, mass, and charge. To test whether mechanical energy is actually conserved, we used a steel marble on a loop-the-loop track. By releasing the marble from the highest point, and calculating the exit velocity, the initial potential energy of the system (PE) and final kinetic energy (KE) of the system should be equal. The experiment did not confirm this prediction. PE was found to be 0.049304 J and average KE was 0.01150 J. Observations of the marble's during its course of motion reveals that energy was dissipated due to the presence of non-conservative forces, namely: friction, vibrations, and air resistance. The average rate of energy dissipation was calculated to be  $3.8 \times 10^{-5}$  J/ms.

## Introduction

The world is built around the concept of energy. Most of the technology we depend on uses some form of energy to be operable. Common forms of energy include: potential, kinetic, electrical, and thermal energy. In order to maintain the energy demands, energy is transformed from one form to another. Experiments have concluded that we cannot simply create energy. Energy must be transformed from one form to another useable form [1]. Antoine Lavoisier discovered a similar phenomenon in the 1700s which is summarized as the law of conservation of mass [2]. In the 1800s Julius Von Mayer restated the first law of thermodynamics; energy cannot be created nor destroyed. This resulted in the principle of conservation of energy [3]. Hydroelectric plants convert KE in water to electrical energy by the use of turbines and generators [4] or solar energy to electrical energy [5]. All of which relies on a source input to generate output.

Energy is not a thing or substance, but a concept that describes in specific terms how fast something is moving, where it is, or how hot it is [6]. KE and gravitational potential energy (PE) are constantly present around us. These energies are fundamental to physics and the natural world and are deeply entwined. PE is associated with a body's tendency or potential to do work. KE is associated with the motion of a body. The goals of this experiment are to: (1) determine the initial height a marble can be released so that it completes a loop and (2) show that the energy in a marble released at  $y=h$  is conserved when the marble is at a point  $y=0$  and is in motion.

## Apparatus

- Steel Marble
- Loop-the-Loop Track
- Meter Stick
- Centimeter Ruler
- Vernier Caliper
- Electronic Balance
- Photogate Timing System

## Procedure

A loop the loop track, illustrated in Figure 1, is constructed from foam pipe. The marble would serve as the medium that transported energy from  $y=h$  to  $y=0$ . The marble was re-released repeatedly from arbitrary heights until it was able to complete a loop. This height was then compared to the theoretical height (Equation 2) which was derived from the conservation of mechanical energy principle (Equation 1). Choosing the highest point on the track to be the initial release point, the PE was calculated. To determine how much of PE was converted to KE, the final velocity of the marble was required. Using two photogates separated by a small distance,  $d$ ; the time difference,  $t$ , from photogate 1 (P1) and photogate 2 (P2) could be measured. The velocity was then calculated by using the relationship between distance and time. The process was repeated 150 times ( $n=150$ ), KE was then calculated (Equation 4) from the average velocity over a total of 150 trials.

$$U_1 + K_1 = U_2 + K_2 \quad (1)$$

$$y_{min} = \frac{27}{10}R_l \quad (2)$$

$$U = mgh \quad (3)$$

$$K = \frac{7}{10}m \left( \frac{d}{t_{avg}} \right)^2 \quad (4)$$

U, potential energy; K, kinetic energy;  $R_l$ , radius of the loop; h, height of the initial release point;  $v_{avg}$ , average velocity; and  $t_{avg}$ , average time. Equation 4 includes the marble's moment of inertia.

Table 1: Initial calculated and measured physical quantities for the experiment

Physical Quantity	Value
Mass of marble (g)	8.3850
Predicted height of release (cm)	29.7
Actual height of release (cm)	46.5
Initial height of release (cm)	46.5
Loop Radius (cm)	11.0
Distance between photogates (cm)	3.922
Initial Potential Energy (J)	0.049

The average time interval used to calculate the exit velocity was found to be 28.5 ms for 150 trials.

Figure 2 illustrates the interval histogram for 150 trials (n=150).

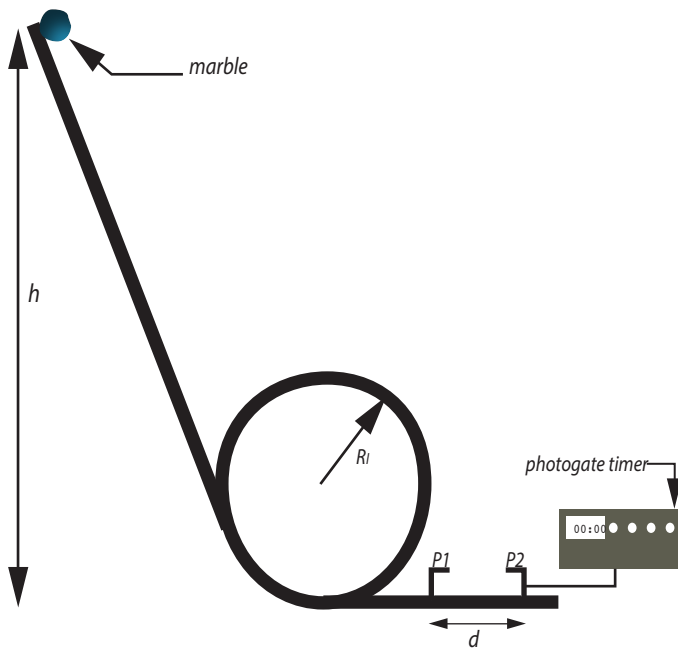


Figure 1: Loop-the-Loop Setup. P1 and P2 indicate the photogate sensor points.

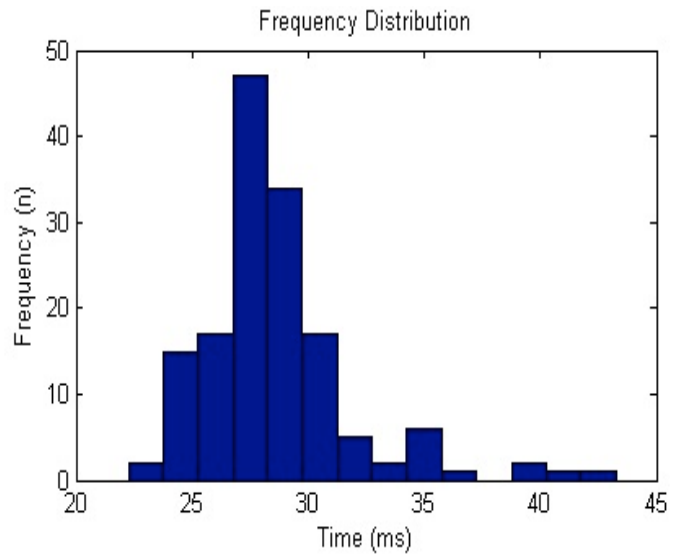


Figure 2: Histogram representation for the time interval between photogates for 150 trials

## Results

Important initial physical quantities are summarized in Table 1. Predicted height of release is based on Equation 2, the actual height of release is the minimum height required to complete a loop, and initial height of release is the height used in the experiment.

Average velocity was calculated to yield 1.393 m/s and the histogram for 150 velocity calculations is shown in Figure 3. KE was calculated to be 0.0115 J. We observed a reduction in final mechanical energy therefore we measured the time interval from  $y=h$  to  $y=0$  for 150 trials to yield an average value of 983 ms. .

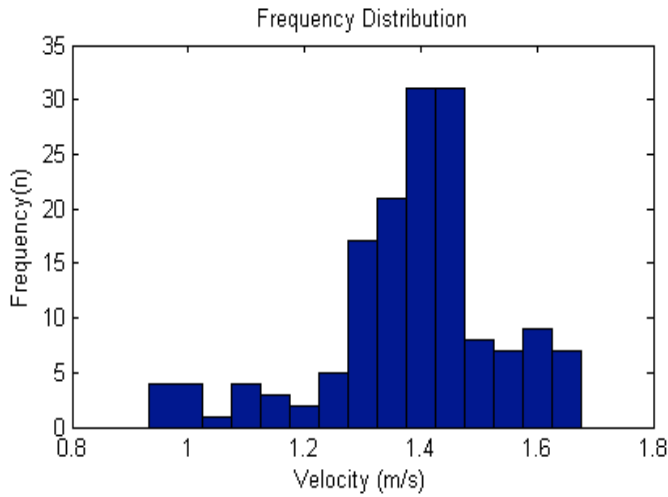


Figure 3:  
Histogram representation for calculated exit velocity

Figure 4 illustrates the histogram for this measurement and Figure 5 shows how mechanical energy changes as a function of time. Given the unpredictability of mechanical energy dissipation, we assumed a linear dissipation.

Calculated values for this experiment is summarized and presented in Table 2.

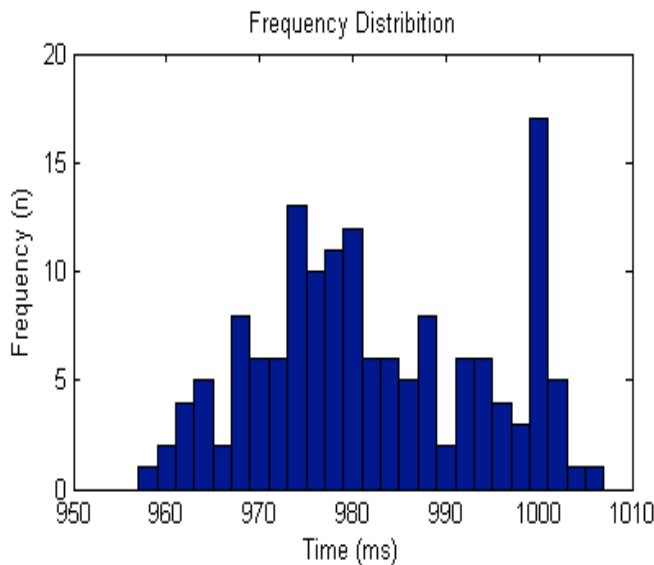


Figure 4:  
Histogram representation for time interval from y=h to y=0.

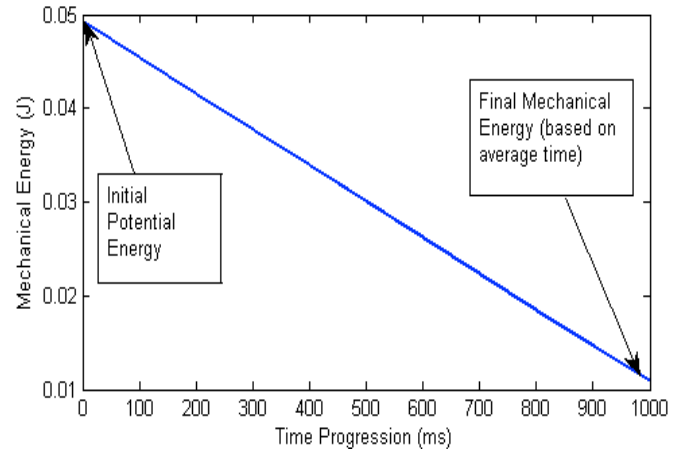


Figure 5:  
Rate of Mechanical Energy Dissipation as a function of time.

Table 2:  
Calculated physical quantities from the experiment

Physical Quantity	Value
$t_{avg}$ (ms)	2.85
$v_{avg}$ (m/s)	1.393
$KE_{avg}$ (J)	0.0115
PE (J)	0.0493
Energy Dissipated (J)	0.0378
Percent Dissipated	76.6
$\Delta PE$ (J)	$8.28 \times 10^{-5}$
$\Delta KE$ (J)	$8.38 \times 10^{-5}$
$\Delta v$ (m/s)	$5.18 \times 10^{-3}$
Rate of Dissipation (J/ms)	$3.5 \times 10^{-3}$

### Error Propagation Analysis

Errors for KE, PE, and v are calculated using partial derivatives with respect to the measured variables. These equations are shown below.  $\Delta$  represents the uncertainty in the measurement; g is the acceleration due to gravity taken as 9.80m/s<sup>2</sup>.

$$\Delta PE = \Delta U = \frac{\partial}{\partial(m, h)} (mgh) = g(m\Delta h + h\Delta m) \quad (4)$$

$$\Delta KE = \frac{\partial}{\partial(m, d, t_{avg})} \left( \frac{7}{10} m \left( \frac{d}{t_{avg}} \right)^2 \right) = \frac{7d}{10t_{avg}^2} \left( 2m\Delta d + d\Delta m + \frac{2dm\Delta t_{avg}}{t_{avg}} \right) \quad (5)$$

$$\Delta v = \frac{\partial}{\partial(d, t_{avg})} \left( \frac{d}{t_{avg}} \right) = \frac{1}{t_{avg}} \left( \Delta d + \frac{d\Delta t_{avg}}{t_{avg}} \right) \quad (6)$$

## Discussion

The marble prior to release was assumed to have no non-conservative forces acting on it. Therefore the total mechanical energy of the system should be conserved and alternating between PE and KE with respect to the marble's x and y position. The relation that defines conservation of energy (Equation 1) should hold. At the top of the incline, the initial starting point,  $U_1 > 0$  and  $K_1 = 0$ . As the marble moved along the track, initial PE is transformed to KE, therefore  $U_p > 0$  and  $K_p > 0$ , where p represents any location between initial and final position. At the final position where  $y = 0$ ,  $U_2 = 0$  and  $K_2 > 0$ . In the ideal closed system,  $U_1 = K_1$  and total mechanical energy is conserved.

Our experimental results does not confirm conservation of mechanical energy, we found  $U_1 > K_2$ . As shown in Table 2, energy values for PE and KE are 0.0493 J and 0.0115 J respectively. KE is approximately one-fourth of PE. Furthermore, the initial theoretical height of release so that the marble completes a loop is less than the actual height of release (see Table 1). Energy errors are in the order of  $10^{-5}$  J and do not explain energy dissipation. With these discrepancies, there had to be some external force acting on the system.

Close observation of the marble in motion reveals that there were external forces also called non-conservative forces acting on the marble. These forces, namely, friction, air resistance, and vibrations decrease the overall energy of a system. At the instant the marble was released these forces were present.

While we could not quantify the individual values of the non-conservative forces, we were able to calculate the rate of energy dissipation. This rate was calculated to be  $3.8 \times 10^{-5}$  J/ms. The presence of non-conservative forces requires an additional term to be added to Equation 1 which then becomes:

$$U_1 + K_1 = U_2 + K_2 + W_0 \quad (8)$$

$W_0$  represents the work done by other forces [7]. In our case  $W_0$  has a value of 0.0378 J (Table 2).

## Conclusion

This experiment demonstrated the principle of conservation of energy in the loop-the-loop and marble system. It was determined through experimentation

that the theoretical release height was much less than the experimental release height. This is a result of non-conservative forces, namely, friction, air resistance, and vibrations decreasing the energy of the system.

From the data calculated, we can conclude that although the values of KE and PE must be the same in a closed ideal system, this idea is not a valid representation of the real world. By adding a variable, in our case,  $W_0$  which accounts for the work done by non-conservative forces,  $K_2 + U_2 + W_0$  must be equal to the initial energy of the system.

Although a large amount of energy was dissipated, a similar experiment using different materials could yield better results. However initial mechanical energy and final mechanical energy will never be the same value. This is because the idea of a frictionless surface is an idealization, like the massless rope; it does not exist in the real world.

## Acknowledgement

We would like to thank our physics instructor, Professor Yoel Rodríguez and our lab technician Mr. Jaime Luján for their help and guidance throughout this project. We would also like to thank our classmates for their continued support.

## References

1. R. D. Knight, Physics For Scientists and Engineers: A Strategic Approach, San Francisco: Pearson Addison-Wesley, 2007.
2. N. J. Tro, Chemistry A Molecular Approach, Upper Saddle River, NJ: Pearson Prentice Hall, 2011.
3. Britannica, "Julius Von Mayer," 2012. [Online]. Available: <http://www.britannica.com/EBchecked/topic/370942/Julius-Robert-von-Mayer>.
4. USGS, "Hydroelectric Power: How It Works," 1 April 2012. [Online]. Available: <http://ga.water.usgs.gov/edu/hyhowworks.html>.
5. W. E. Horne. United States of America Patent 4,313,024, 1982.
6. R. H. Romer, Energy An Introduction to Physics, San Francisco: W.H. Freeman, 1976.

[7] H. D. Young, R. A. Freedman and L. Ford, University Physics, Boston: Pearson Addison-Wesley, 2007.

[8] DOE, "Berkeley Lab Scientists Generate Electricity From Viruses," 13 May 2012. [Online]. Available: <http://newscenter.lbl.gov/news-releases/2012/05/13/electricity-from-viruses/>.

# Cloning and Expression of *CDC13* gene from *Candida parapsilosis*

Ana Rosario

Natural Sciences Department, Hostos Community College, Bronx, New York

**Cdc13 is one of the proteins important in telomere maintenance. Biochemical properties of this protein can be better investigated by isolation of this protein and assessing its catalytic properties in vitro. This work described cloning of *CDC13* gene into the expression plasmid pSMT3 and initial steps of CpCdc13 recombinant protein purification from bacterial cells.**

## Introduction

Proteins are important molecules in eukaryotic and prokaryotic organisms, due to all the function they perform. They are essential part of cellular structures and they act as enzymes - catalysts of biochemical reactions. Antibodies are also made of proteins, so proteins play a significant role in functioning of the immune system. In prokaryotes, production of some proteins contributes to bacterial pathogenicity. In general, proteins are essential part of the survival and development of both prokaryotic and eukaryotic organisms (7). Due to all the functions proteins perform within a cell, they are target of many scientific studies.

Some information about biochemical properties of proteins can be deduced from observation of cells *in vivo*. Isolation of a protein and analyzing its biochemical properties *in vitro* in the laboratory is another way to study proteins. This approach usually yields more information about structure and enzymatic properties of proteins than study of live cells.

Telomeres are non-coding DNA regions at the end of linear chromosomes in eukaryotic cells. Telomeric DNA consists of simple repetitive sequences, and has a single-stranded overhang at its 3' end. Telomeres prevent DNA from shortening after successive rounds of replication, and preserve the genome by protecting genes essential for life. (1, 4).

Cdc13p is single-stranded DNA binding protein, which has an important role in maintenance of telomeres. It was proposed that Cdc13 has a role in telomere protection (2, 3).

The goal of this laboratory project was to compare

biochemical properties of Cdc13 from different *Candida* species. This work describes isolation of Cdc13p from *C. parapsilosis*, which was the first step in this project.

## Materials and Methods

### *Isolation of genomic DNA (Smash and Grab).*

Genomic DNA from *Candida parapsilosis* was isolated using modification of the *Smash and Grab* methods. *C. parapsilosis* cells were inoculated in 5 ml of YEPD and grown overnight at 30°C. Cells were collected by centrifugation for 10 minutes at 1500 rpm, washed with 1 ml of water, and resuspended in 300 µl of breaking buffer (2 % (v/v) Triton X-100, 1 % (v/v) SDS, 100 mM NaCl, 100 mM TrisCl, PH 8.0, 1 mM EDTA, pH 8.0). The suspension was mixed with 250 µl of glass beads and 300 µl of Phenol-Chloroform-Isoamyl mix (PCI) and vortexed for 20 minutes in the cold room. The resulting suspension was centrifuged for 10 minutes at 14000 rpm. The upper fraction containing genomic DNA was collected, and DNA was precipitated with ethanol. DNA precipitate was resuspended in 400 µl of TE buffer (10 mM Tris/HCl, pH 7.5, 1 mM EDTA, pH 8.0), to which 10 µg of RNase was added to digest residual RNA in the the DNA preparation. The sample was subjected to additional PCI treatment as described above. DNA was precipitated with ethanol and re-suspended in 50 µl of TE buffer. This preparation was analyzed by agarose gel electrophoresis (Figure 2) and used as a template in PCR reaction (5).

### *Polymerase Chain Reaction (PCR).*

Polymerase chain reaction was performed as described before (5).

Briefly, 1 µl of *C. parapsilosis* genomic DNA, 2 µl of 10 mM MgCl<sub>2</sub>, 1 µl of 10 mM dNTP mix, 1 µl of 100 ng/µl of CparCDC13-F-SacI primer, 1 µl of 100 ng/µl of CparCDC13-R-XhoI primer, 1 µl of Herculanase polymerase, 5 µl of 10 x PCR reaction buffer supplied by manufacturer, and 40 µl of water were mixed in 0.5 ml PCR tube. Tubes were placed in the Thermo-cycler, and PCR cycles were set as follows: 5 minutes at 94°C to denature template DNA, followed by the thermocycle: 94°C for 1 minute, 50°C for 1 minute, 72°C for 2 minutes, for total of 30 cycles. After completion of 30 cycles, the product was allowed to anneal for additional 10 min at 72°C, and reaction was cooled down to 4°C. PCR products were analyzed the agarose gel electrophoresis (Figure 3).

#### *Cloning of the gene into the plasmid vector.*

DNA obtained by PCR (CpCDC13 DNA) and pSMT3 plasmid vector were treated with restriction nucleases in a reaction that contained 10 µg of DNA, 5 µl of the appropriate restriction buffer supplied by the manufacturer, and 0.5 µl of SacI and XhoI restriction enzymes in 20 µl digestion reaction. Products of the reaction were analyzed by gel electrophoresis and purified using DNA purification kit (BioBasics). About 5 µg of the digested PCR product and 0.8 µg of the digested pSMT3 DNA were mixed with 1 µl of 1 mM ATP, 1 µl of T4 DNA ligase, and 1 µl of T4 DNA ligase buffer supplied by manufacturer in 10 µl reaction. The reaction mixture was incubated at 16°C overnight followed by heating to 65°C for 10 minutes to inactivate the DNA ligase.

#### *Bacterial transformation.*

For bacterial transformation, 5 µl of ligation reaction mix was incubated with 50 µl of competent BL21 codon + *E. coli* cell on ice for 30 minutes. This mixture was heat-shocked at 42°C for 45 seconds and cooled on ice for 2 minutes. After adding 450 µl of SOC media, cells were allowed to recover at 37°C for 1 hour and plated on LB media supplemented with 50 µg/ml of kanamycin. Plates were incubated at 37°C overnight, and 14 transformants were selected for further analysis (Figure 4).

#### *Protein induction*

Three colonies of transformants were inoculated in 20 ml LB medium supplemented with 50 µg/ml of kanamycin and incubated at 37°C overnight. 15 ml of this overnight culture was inoculated into 1 liter of LB medium supplemented with 50 µg/ml of kanamycin

to a final optical density of culture (OD<sub>600</sub>) of 0.1. Cultures were incubated at 37°C until OD<sub>600</sub> reached 0.5 (about 2.6 hrs). Culture were chilled on ice for 30 minutes and protein expression was induced by addition of 200 mM IPTG up to final concentration of 0.1 mM and 100% EtOH up to final concentration of 2%. Induced cultures were incubated at 16°C overnight. Cells were collected by centrifugation at 6000 rpm for 10 min at 4°C and re-suspended in 20 ml of Buffer E (50 mM Tris-HCl pH 7.5, 250 mM NaCl, 10% glycerol, 1 mM PMSF, 1 µg/ul pepstatin, 1 µg/ul leupeptin). Bacterial cell walls were digested by addition of lysozyme up to the final concentration of 0.2 mg/ml. After chilling on ice for 30 minutes, cells were lysed by addition of 10% Triton (final concentration of 0.1%) and incubated for additional 15 minutes on ice. Cells were sonicated using a Branson Sonifier 250 set up for 30% duty cycle, output 5, 10 minutes at 4°C. Sonicated cultures were centrifuged at 32,000 rpm for 1 hour at 4°C in Sorvall T865 titanium ultracentrifuge rotor to pellet cell debris. Cell lysate was collected by pipetting and stored at -80°C (Figure 6).

#### *Protein Purification*

Protein lysate was removed from -80°C and thawed in ice-cold water. Ni-NTA agarose beads were equilibrated by washing resin 3 times in buffer E (50 mM Tris-HCl pH 7.5, 250 mM NaCl, 10% glycerol), pH 7.5. Protein extract was mixed with washed Ni-NTA resin and incubated at 4°C with rotation for 30 min to allow for resin-protein binding. Ni-NTA beads bound protein was washed with buffer E supplemented with 25 mM and 100 mM imidazole solutions respectively. Protein was eluted with buffer E supplemented with 300 mM imidazole solution and collected in 0.5 ml fractions. Protein concentration was determined by Bradford assay (BioRad), protein quality was assessed by SDS/PAGE. Eluate fractions 1 and 2 containing highest protein amount were combined for further purification (Figures 7, 8, 9)

## **Results**

Methods used in this project to isolate and obtain a large amount of the target protein Cdc13 from the fungus *Candida parapsilosis* were DNA cloning and recombinant DNA technology. One of the most important tools for cloning a gene is a cloning vector. A cloning vector is a modified circular plasmid DNA able to self-replicate within a host cell. The cloning vector used for cloning of CDC13 was pSMT3 (3). This vector



allows for inducible expression of a cloned gene and for selection of transformed competent cells on media supplemented with antibiotic kanamycin. The plasmid vector also carries DNA sequences that encodes a string of histidines called a His-tag. The His-tag is expressed as a part of a recombinant protein. Its function is to aid in purification of a protein by chromatography. pSMT3 vector also includes an origin of replication site (ori), which is essential for plasmid replication in a cell (Figure. 1).

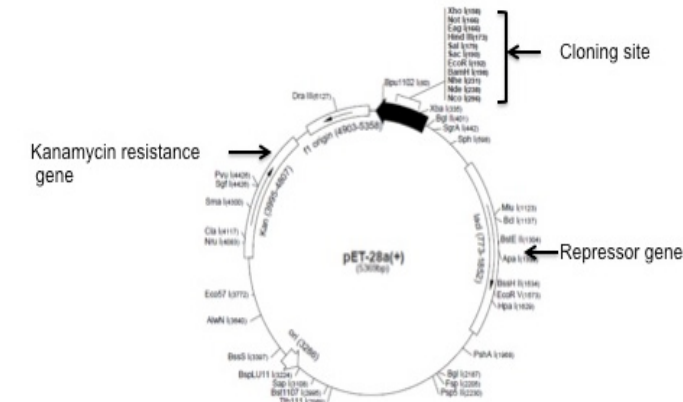


Figure 1  
Genetic map of the expression vector pSMT3

Before *CDC13* gene can be cloned into the pSMT3 vector, *CDC13* DNA was amplified out of genomic DNA. The first step in this procedure was to isolate the genomic DNA from fungus *C. parapsilosis* by using *Smash and Grab* method (see Materials and Methods). To verify quality of the preparation, isolated genomic DNA was subjected to gel electrophoresis in agarose gel (Figure 2).

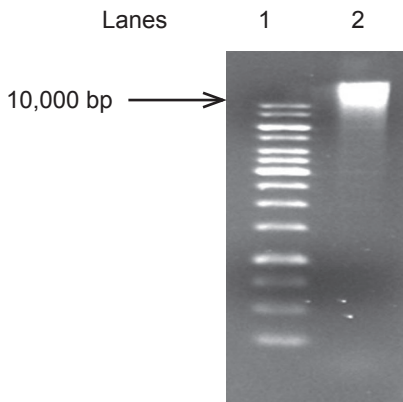


Figure 2  
Isolation of *C. parapsilosis* genomic DNA  
5  $\mu$ l of genomic DNA from *C. parapsilosis* was loaded on 0.7% agarose gel and subjected to electrophoresis.

Lane 1: DNA molecular weight marker  
Lane 2: *C. parapsilosis* genomic DNA.

PCR reaction is a way of amplifying the sequence of interest out of a larger DNA molecule by using small single-stranded oligonucleotides complimentary to 5' and 3' ends of a target DNA sequence as primers for DNA polymerization. The role of these primers is to initiate DNA replication. DNA polymerase acts by adding new nucleotides to 3' end of a primer to form a new complementary DNA strand. The amplification of the gene is accomplished in three steps: first, DNA template is denatured; second, primers anneal to template strands; and third, the DNA polymerase extends the new strand by adding new nucleotides to the 3' end of the primer. Amount of DNA produced in PCR reaction increases exponentially over time. After the PCR was performed, a small sample of PCR products was subjected to an agarose gel electrophoresis to verify *CDC13* amplification. (Figure 3). The expected size of *CDC13* was approximately 1400 kb (kilobases). As can be seen on Figure 3, the single band of PCR product corresponds DNA of this size.

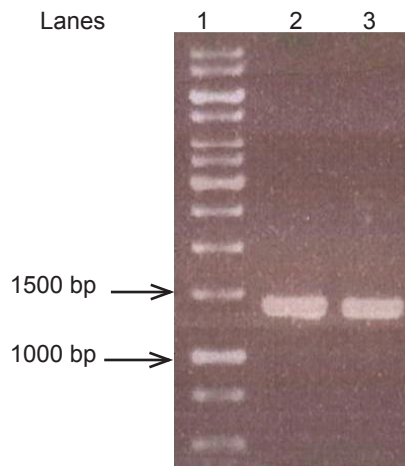


Figure 3

Agarose electrophoresis of PCR products  
Lane 1: DNA molecular weight marker  
Lane 2: PCR product from the reaction 1  
Lane 3: PCR product of reaction 2

5  $\mu$ l of each PCR reaction was loaded on 0.7% agarose gel and subjected to electrophoresis

In order to clone the *CDC13* gene into the pSMT3 vector, both vector and *CDC13* PCR product were digested with the same restriction enzymes, *SacI* and *XhoI* (Materials and Methods). The role of these restriction enzymes was to cut both DNA molecules inside the specific sequences at the 5' and 3' DNA ends. Thus, complementary sticky ends in *CpCDC13* and pSMT3 DNA fragments were created. Digested *CDC13* and pSMT3 were subjected to agarose gel electrophoresis to separate DNA fragments resulted from digestion.

DNA bands corresponding to the *CDC13* insert and pSMT3 vector DNA were cut out from agarose gel and purified. Thus, DNA fragments were prepared for ligation.

The purpose of ligation reaction was to form a recombinant DNA molecule pSMT3 *CpCDC13* by inserting *CpCDC13* gene into the cloning site of the pSMT3 (Materials and Methods). T4 DNA ligase is an enzyme capable of creating a covalent diphosphate bond between the sticky ends of DNA molecules.

Amount of the digested insert (*CpCDC13* DNA) and vector (pSMT3 DNA) was verified by agarose gel elec-

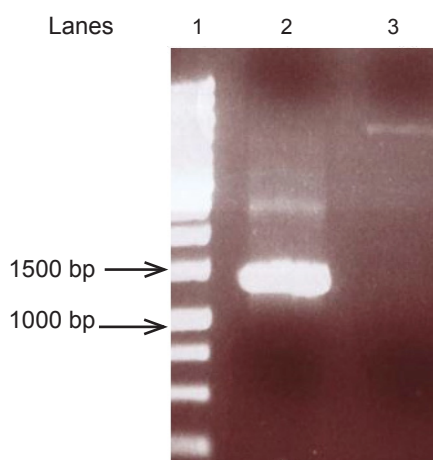


Figure 4:

Agarose gel electrophoresis of insert and vector DNA fragments. *CpCDC13* PCR product and plasmid vector pSMT3 were digested with *SacI/XhoI* restriction endonucleases, resolved by agarose gel electrophoresis, and extracted from agarose. 5  $\mu$ l of purified *CpCDC13* DNA fragment (insert) and 5  $\mu$ l of purified pSMT3 DNA (vector) were subjected to agarose gel electrophoresis to verify relative DNA concentration.

Lane 1: Molecular weight marker

Lane 2: 5  $\mu$ l of purified *CpCDC13* DNA fragment (insert)

Lane 3: 5  $\mu$ l of purified pSMT3 DNA (vector)

Ratio of *CpCDC13* and pSMT3 DNA used for ligation reaction was 6:1. Ligation reaction was incubated overnight at 16°C, and heating reaction mixture for 10 minutes at 65°C after the completion of the reaction inactivated T4 DNA ligase. Half of the ligation reaction was used for transformation competent *E. coli* DH5 $\alpha$  cells (see Materials and Methods). Transformants were plated on LB/Kan plate, incubated overnight, and 14 colonies were selected for analysis of integration. This was done by first growing selected transformants in LB/Kan broth overnight followed by purification of

plasmid DNA from cells. Isolated plasmids were subjected to restriction digest with *XhoI* and *SacI* and resulting restriction fragments were analyzed by agarose gel electrophoresis. DNA fragments expected from digestion of recombinant plasmids were 1400 bp for the insert and 5664 bp for the vector. As can be seen from Figure 5, only clones # 2, 11, 12, and 13 contained both vector and insert. The rest of analyzed plasmids were just empty vectors. Clones # 2, 11, 12, and 13 were selected for further analysis (Figure 5).

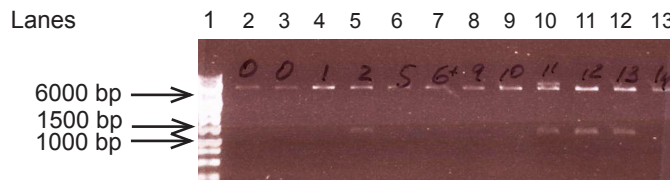


Figure 5:

*SacI/XhoI* digest of the recombinant transformant.

Ligation reaction products were transformed into *E. coli* DH5 $\alpha$  cells and plated on LB/Kan plate. 12 transformant colonies were inoculated into LB/Kan media and grown to saturation. Plasmid DNA from these cultures was isolated and digested with *SacI/XhoI* restriction nucleases. Products of the digest were separated through electrophoresis in agarose gel.

Lane 1: Molecular weight marker

Lanes 2-13: *SacI/XhoI* restriction digest of the recombinant plasmids.

The next step in this project was to verify whether the protein expression from the recombinant plasmid could be induced. Recombinant plasmids pSMT3*CpCDC13* clones 2, 12, 13, were transformed into *E. coli* expression strain BL21codon+. Cell cultures were grown to an exponential phase, and protein production was induced by addition of IPTG and Ethanol (see Materials and Methods). Transcription of *CDC13* from the recombinant plasmid was under control of *Lac* operator. The *Lac* operator is a DNA sequence to which the lac repressor binds. Binding of lac repressor obstructs transcription from a downstream promoter, a DNA sequence to which the RNA polymerase binds. Once IPTG binds to the lac repressor, the repressor dissociates from the promoter site allowing the RNA polymerase to bind to the promoter site and to start transcription. To verify induction of a protein, aliquots of culture before and after IPTG induction were collected. Cells were pelleted and boiled for 5 minutes in Laemmli buffer to release cell content. Protein samples were loaded on 10% polyacrylamide gel and resolved by electrophoresis (PAGE). To visualize protein bands, the gel was stained with Coomassie blue dye that stains proteins in the gel in a blue color (Figure 6).

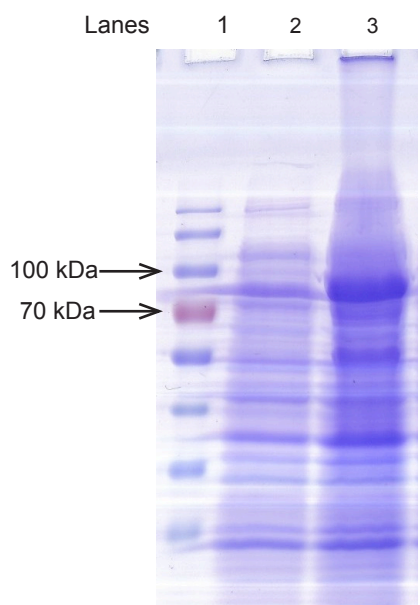


Figure 6:  
Induction of CpCdc13 from the recombinant expression plasmid.

Lane1: Molecular weight marker  
Lane 2: CpCdc13 expression in uninduced cells  
Lane 3: protein expression in induced cells.

As can be seen on Figure 6, the protein band corresponding to CpCdc13 protein obtained from cells after induction (lane 2) is considerably wider as compared to protein band obtained from cells before induction (lane 3). This verifies that more of Cdc13 protein was produced after induction, e.g. that protein expression from the recombinant plasmid was induced. The next step of the project was to isolate protein in quantities sufficient for its biochemical analysis. *E. coli* culture was prepared as described in Materials and Methods. Cells were collected by centrifugation and cell wall was digested by addition of lysozyme. Cells were lysed by addition of the detergent, Triton-X, followed by sonication, a process that breaks cells. When cell structures were destroyed, proteases released by cell destruction could degrade other proteins in cell lysate including the protein of interest (CpCdc13). To prevent proteins from degradation, protease inhibitors were added to cell lysate before sonication. Cell lysate was centrifuged to separate solid cell particles from soluble proteins. The next step in protein isolation was separation of the target protein CpCdc13 from other proteins. The target protein was expressed with histamine tag, which has high affinity to metal ions such as Nickel. This feature of the protein was exploited in using Ni-NTA agarose resin to aid in separation of CpCdc13 from a protein mixture. Ni-NTA agarose resin is a suspension of very small beads made of agarose and covered in Ni ions. Protein lysate was mixed with Ni-NTA resin, and CpCdc13p was allowed to bind to Ni-NTA beads.

The Protein-Ni-NTA resin suspension was loaded on a small plastic column with a tap on the bottom. The flow through the column contained proteins which were not bound to Ni-NTA resin. Imidazole promotes dissociation of proteins from the Ni-NTA resin. As some proteins may naturally have a low affinity to Nickel ions, the resin was first washed with solutions containing low concentration of imidazole. The first wash was made with 25mM of Imidazole. The protein mixture obtained from this wash was collected in one tube. The second wash was made with 100 mM of Imidazole. The protein mixture obtained from this wash was collected in three 1 ml fractions. Using different low concentrations of Imidazole allowed to wash out proteins with no specific binding and with low affinity from the column (Figure 7).

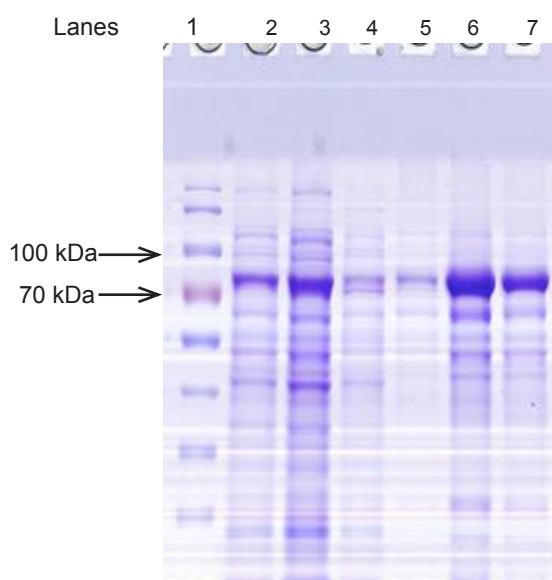


Figure 7:  
Binding of CpCdc13 to Ni-NTA agarose and column wash. 3µl of each sample of protein solution was resolved on SDS-PAGE  
Lane1: Molecular weight marker  
Lane 2: protein lysate  
Lane 3: flow through  
Lane 4: Wash with 25 mM Imidazole  
Lane 5: Wash with 100 mM Imidazole, fraction1  
Lane 6: Wash with 100 mM Imidazole, fraction2  
Lane 7: Wash with 100 mM Imidazole, fraction3 Elution fraction were collected, and 3µl of protein solution from each fraction was resolved on denaturing polyacrylamide gel.

To elute the target protein, higher Imidazole concentration (300 mM) was used. CpCdc13 eluted from the column was collected in six fractions and analyzed by SDS-PAGE (Figure 8). Concentration of partially purified CpCdc13 was measured by Bradford assay. This assay measures the concentration of protein by using Coomassie Brilliant Blue dye. When Coomassie Brilliant Blue is added to the protein solution, color of the dye changes. Intensity of the color change depends

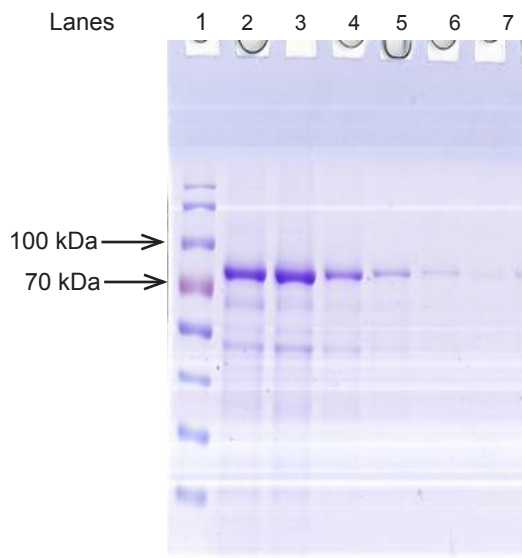


Figure 8:  
Elution of CpCdc13 from Ni-NTA agarose column. Elution fraction were collected, and 3 $\mu$ l of protein solution from each fraction was resolved on 10% SDS-PAGE.

Lane 1: Molecular weight marker  
Lane 2: 300 mM Imidazole fraction 1  
Lane 3: 300 mM Imidazole fraction 2  
Lane 4: 300 mM Imidazole fraction 3  
Lane 5: 300 mM Imidazole fraction 4  
Lane 6: 300 mM Imidazole fraction 5  
Lane 7: 300 mM Imidazole fraction 6

on protein concentration in the solution. These changes can be analyzed by measuring the optical density of Coomassie Blue/protein solution in spectrophotometer at wavelength of 595 nm. To establish the relationship between the protein concentration and the OD<sub>595</sub> of the Coomassie blue/protein solution. First, optical density of Coomassie blue solution mixed with the solution of Bovine Serum Albumin (BSA) of known concentration was measured. Data obtained from these measurements allowed for establishing a correlation between optical density at OD<sub>595</sub> and protein concentration. (Figure 9). Data was plotted in Excel and slope equation was calculated. Then, different fractions of protein collected from protein purification were also mixed with Coomassie Blue dye and OD<sub>595</sub> of solutions were measured. To calculate amount of the protein in each fraction, correlation established between known amount of protein and OD<sub>595</sub> was applied (Table 1).

## Discussion

Isolation and purification of the protein of interest is required to gain more information about its biochemical properties. However, it is just the first step in characterization of protein biochemical properties.

Table 1  
Calculation of protein concentration using Bradford Assay

mg/ml	BSA OD 595	Cdc13-tag sample	OD 595	mg/ml	mg/ml
2	0.0899	PT	0.317	12.477273	
4	0.1299	PT	0.472	19.522727	1.9522727
6	0.1732	5mM Im	0.507	21.113636	2.1113636
8	0.2181	100mM-1	0.512	21.340909	2.1340909
10	0.2631	100mM-2	0.614	25.977273	2.5977273
12	0.3081	100mM-3	0.658	27.977273	2.7977273
		300mM-1	0.676	28.795455	2.8795455
		300mM-2	0.677	28.840909	2.8840909
		300mM-3	0.654	27.795455	2.7795455
		300mM-4	0.621	26.295455	2.6295455
		300mM-5	0.59	24.886364	2.4886364
		300mM-6	0.562	23.613636	2.3613636

Table 1:  
Protein concentration of protein solutions obtained from washing and elution of CpCdc13 bound to Ni-NTA column was calculated using Bradford Assay. Standard curve constructed for the purpose of establishing a mathematical relationship between optical density at 595 nm and protein concentration is depicted below (Figure 9).

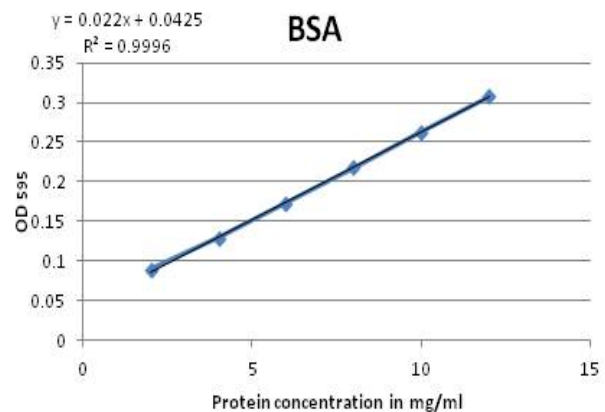


Figure 9:  
Standard curve.  
Standard curve was constructed from data received from measuring optical density of Bovine Serum Albumin solutions of known concentration (Table 1).

Gene cloning, protein induction and purification procedures will be repeated to clone *CDC13* from others species of *Candida*, such as *C. lusitaniae* and *C. guilliermondie*. Once the recombinant Cdc13 proteins from the different *Candida* species are isolated, they will be analyzed to study and compare their properties and functions. Thus, it will allow for establishing differences and similarities among them.

## Acknowledgement

The author would like to thank Dr. Neal Lue for the opportunity to intern in his laboratory and Dr. Olga Steinberg Neifach for guidance and support. This material is based upon work supported by the National Science Foundation under Grant No. MCB-1157305 to N.F. Lue and O. Steinberg Neifach

## References:

1. Blackburn, E.H. (1991) Telomeres. *Trends in Biochemical Sciences*, 10:378-381.
2. Evans, S. K., and V. Lundblad. (1999). Est1 and Cdc13 as co-mediators of telomerase access. *Science* 286:117–120
3. Garvik, B., M. Carson, and L. Hartwell. (1995) Single-stranded DNA arising at telomeres in *cdc13* mutants may constitute a specific signal for the RAD9 checkpoint. *Molecular and Cellular Biology*. 15:6128-6138
4. Greider C.W. 1991 Telomeres. *Current Opinions in Cell Biology* 3:444-451
5. Harth, G. And M.A. Horwitz (1997). Expression and Efficient Export of Enzymatically Active *Mycobacterium tuberculosis* Glutamine Synthetase in *Mycobacterium smegmatis* and Evidence that the Information for Export is Contained within the Protein. *The Journal of Biological Chemistry*, 272: 22728–22735.
6. Molina, A. and O. Steinberg, (2010). Construction of the disruption cassette for the deletion of the EST3 gene in *C. parapsilosis*. *Hostos Journal of Student Research*, 2: 7-14. Retrieved from October 2, 2013 from [http://www.hostos.cuny.edu/oaa/nas/pdfs/HJSR\\_2.pdf](http://www.hostos.cuny.edu/oaa/nas/pdfs/HJSR_2.pdf)
7. Tortora, G., Funke, B., & Case, C. (2010). *Microbiology: An introduction*. (10th ed.). San Francisco, CA: Benjamin-Cummings Pub Co.



Ms. Rosario sets up an experiment at the laboratory of the Weill Cornell Medical College.

## CpCdc13 Interaction with *Candida parapsilosis* and *Candida lusitania* Telomeres

Eliana Perez

Natural Sciences Department, Hostos Community College, Bronx, New York

**Specificity of Cdc13p binding to *Candida* telomeres is currently a topic of much debate. We have investigated binding of Cdc13p isolated from *Candida parapsilosis* to telomeric repeats of *Candida parapsilosis* and the related *Candida* specie *Candida lusitania*. Our data demonstrated that CpCdc13 binds specifically to telomeric repeats of both related *Candida* species.**

### Introduction

Telomeres are nucleoproteins structures located at the end of linear eukaryotic chromosomes. Telomeres are composed of genomic DNA, telomere-associated proteins, and RNA. Telomeric DNA consists of several double-stranded, non-coding DNA repeats that end up in a 3' single stranded, guanine-rich (G-rich) overhang. Primary and crucial functions of telomeres are to protect genome integrity and maintain chromosomal stability. Telomeres can perform this function by preventing DNA degradation and maintaining telomeric DNA length. The length of telomeres is maintained by a specialized nucleoprotein complex called telomerase. This complex acts as a reverse transcriptase, which makes possible for it to add nucleotides to the 3' end of single stranded telomeres using an associated RNA subunit as a template. Telomerase is a conserved complex; homologs of it have been found in the majority of eukaryotic organisms (1, 4).

A large number of telomere-associated proteins aid telomere maintenance and support telomeres structural integrity. In yeast, the CST complex containing Cdc13, Stn1, and Ten1 proteins, binds to single-stranded G-rich telomeric repeat. Cdc13 function is to protect and stabilize telomeres, and regulate telomere maintenance (2, 3, 6). Initially, it was thought that CST-complex proteins are a part of the fungi-specific telomerase regulation only. However, proteins that are believed to be orthologues of CST were recently discovered in other eukaryotic organisms such as fungi, plants and mammals (6, 8, 9).

Cdc13 orthologues were identified through bioinformatics searches. Amino acid composition and partial structures of putative Cdc13p orthologues greatly vary

from specie to specie. The Cdc13-like functions of putative Cdc13p orthologues were also demonstrated using genetics methods. Mutation in putative *CDC13* results in the telomere-capping defect similar to the one associated with loss of specific Cdc13p functions in yeast. Whether or not all of the Cdc13 proteins have similar biochemical properties is not clear yet, as investigators from various laboratories reported somewhat contrary results. For example, Mandell et. al. reported that Cdc13 from various *Candida* species do not exhibit high DNA binding specificity characteristic of *S. cerevisiae* Cdc13 (5). Somewhat different data were reported by Yu et al., who demonstrated that *C. tropicalis* Cdc13 binding to telomeric DNA is specific. DNA binding specificity of Cdc13 from other *Candida* species have not yet been investigated (9).

Biochemical properties of *C. tropicalis* Cdc13 were investigated previously. It was demonstrated that high affinity binding of CtCdc13 to telomeres requires a long telomeric DNA sequence and that dimerization through the OB4 domain of the protein is important for this reaction. *C. parapsilosis* is a *Candida* specie distantly related to *C. tropicalis*. Telomeric sequence of *C. parapsilosis* and amino acid sequence of CpCdc13 differ from those of *C. tropicalis* and *C. albicans*. In this work we sought to express and purify recombinant CpCdc13 in order to assess its biochemical properties, telomeric DNA binding in particular, and compare it to that of other *Candida* species. The resulting data will allow determination of whether the mechanism of Cdc13-DNA binding is similar in distantly related *Candida* species.

## Materials and Methods

### *Introduction of plasmid into competent cells*

DH5- $\alpha$  competent cells were transformed with recombinant plasmid pSMT3CpCDC13, which carried *CDC13* gene under control of *Lac* promoter as described earlier (7). Briefly, 1  $\mu$ g of plasmid was incubated with 100  $\mu$ l of competent cells for 30 minutes on ice followed by heat shock for 45 seconds at 42°C. Cells were allowed to recover for 2 minutes on ice before addition of 900  $\mu$ l of SOC medium and were further incubated at 37°C water bath for 1 hour. Out of this transformation reaction, 50  $\mu$ l were plated on each of two LB plates supplemented with 50  $\mu$ g/ml of kanamycin and incubated at 37°C overnight.

### *Induction of protein*

Three colonies of transformants were inoculated in 20ml LB medium supplemented with 50  $\mu$ g/ml of kanamycin and incubated at 37°C overnight. 15ml of overnight culture was inoculated into 1L of LB medium supplemented with 50  $\mu$ g/ml of kanamycin to final density of OD<sub>600</sub> of 0.1 and incubated at 37°C until OD<sub>600</sub> of the culture reached 0.5 (about 2.6 hrs). The culture was chilled on ice for 30 minutes and protein expression was induced by addition of 200mM IPTG to the final concentration of 0.1 mM and 100% EtOH to the final concentration of 2%. This culture was incubated at 16°C overnight. Cells were collected by centrifugation at 6000 rpm for 10 minutes at 4°C and re-suspended in 20 ml of Buffer E (50 mM Tris-HCl pH 7.5, 250 mM NaCl, 10% glycerol, 1 mM PMSF, 1  $\mu$ g/ $\mu$ l pepstatin, 1  $\mu$ g/ $\mu$ l leupeptin). After that, lysozyme was added to the final concentration of 0.2 mg/ml. Culture was incubated on ice for 30 min before adding 10% Triton to the final concentration of 0.1% and incubated further for additional 15 minutes. Cells were sonicated using Branson Sonifier 250 set up for 30% duty cycle, output 5, 10 minutes at 4°C. Sonicated culture was centrifuged at 32,000 rpm for 1 hour at 4°C in Sorvall T865 titanium ultracentrifuge rotor to pellet cell material. Cell extract was collected by pipetting and stored at -80°C

### *Protein Purification*

Protein extract was removed from -80°C and thawed in ice-cold water. Ni-NTA agarose beads were equilibrated by washing resin 3 times in buffer E (50 mM Tris-HCl pH 7.5, 250 mM NaCl, 10% glycerol), pH 7.5. Protein extract was mixed with washed Ni-NTA resin and incubated at 4°C with rotation for 30 minutes to induce resin-protein binding. Resin was washed with buffer E supplemented with 25 mM and 100 mM imidazole solutions respectively. Protein was eluted with

buffer E supplemented with 300 mM imidazole and collected in 0.5 ml fractions. Protein concentration was determined by Bradford assay (BioRad), protein quality was assessed by SDS/PAGE. Eluate fractions 1 and 2 containing highest protein amount were combined for further purification.

### *Bradford assay to determine protein concentration*

Protein concentration was determined by the Bradford assay. Bradford reagent (BioRad) was diluted 1:5 with distilled water and 1 ml of the diluted reagent was mixed with 1  $\mu$ l of a protein solution. Optical density of this solution was determined at a wavelength of 595 nm. Solutions of Bovine Serum Albumin (BSA) of known concentrations were used to construct the standard curve and calculate the relationship between protein concentration and optical density of a solution.

### *HIS-SUMO-Tag removal*

Protein samples from earlier steps were combined as described above and dialyzed against buffer E to remove imidazole. The resulting protein was digested with UPL1 protease (2  $\mu$ g/ $\mu$ l) for 3 hours on ice. The digested His-tag was separated from the protein of interest by additional purification through Ni-NTA agarose. Digested protein was mixed with equilibrated Ni-NTA resin, incubated at 4°C with rotation for 1 hour, loaded on a column, and allowed to drain by gravity. Protein was eluted with buffer E supplemented with 50 mM imidazole and collected in 0.6 ml fractions. Protein concentration was determined by Bradford assay (BioRad), and protein quality was assessed by SDS/PAGE.

### *Gel mobility shift assay*

Binding reaction was set up in assay buffer (50 mM Tris-HCl, pH 8.0, 1 mM MgCl<sub>2</sub>, 1mM spermidine, 1 mM DTT, 5% glycerol). CpCdc13 was mixed with P<sup>32</sup> labeled telomeric *C. paprapasilosis* TEL GX2 DNA probe representing two *C. paprapasilosis* telomeric repeats. Additionally, 20 to 100ng of cold telomeric CpGX2 oligonucleotide (GGTCCGGATGTTGATTTATACT-GAGGTCCGGATGTTGATTTATACTGA) or the same amount of P<sup>32</sup> labeled and cold *C. lusitania* TEL GX2 oligonucleotide telomeric repeats (CTGATGTTCTTTAG-GGAGGTA CTGATGTTCTTTAGGGAGGTA) was introduced into the mixture. The resulting protein-DNA complexes were resolved by native acrylamide gel electrophoresis. Acrylamide gel was dried on 3 MM paper and exposed on Phosphor screen overnight (GE). The resulting image was scanned on Typhoon PhosphorImager and analyzed using ImageQuant software. (Molecular Dynamic).

## Results

To compare biochemical properties of Cdc13 from different candida species, Cdc13 proteins from related *Candida* species, *Candida tropicalis* and *Candida parapsilosis*, were isolated and characterized. Biochemical properties of Cdc13 from *Candida tropicalis* were described earlier (8). This work describes isolation and characterization of Cdc13 from *Candida parapsilosis*.

Cloning of *CpCDC13* into pSMT3 vector was described earlier (7). The resulting plasmid pSMT3-*CpCDC13* was transformed into DH5- $\alpha$  *E. coli* cells. Transformed cultures were grown to exponential phase at 37°C, and protein expression was induced by addition of 0.1 mM IPTG and 2% ethanol. Cultures were allowed to grow for additional 16 hours and were collected by centrifugation. Protein lysate was prepared as described in Materials and Methods. Briefly, cells were re-suspended in buffer E, chilled on ice and treated with 0.2 mg/ml lysozyme to cleave the peptidoglycan cell wall. Additionally, Triton X-100 detergent was added to final concentration of 0.1% to promote solubilization of cell structures. After additional 15 minutes of incubation on ice, cell suspension was subjected to sonication to break down cells. Cell lysate resulting from sonication was transferred to centrifuge tubes, and subjected to centrifugation for 1 hour, at 34,000 rpm at 4°C in order to separate cell debris and proteins. Supernatant containing protein extract was collected, frozen in liquid nitrogen, and was kept at -80°C until the next step in purification.

Induction of *Lac* promoter from pSMT3-*CpCDC13* plasmid allowed for expression of the histidine-tagged protein of interest. Presence of the histidine tag as a part of the induced protein was used to further purify the tagged protein on Ni-NTA resin. Ni-NTA resin contains agarose beads covered in positively charged Ni-containing complex, which binds to the histidine tag carried by the protein. Purification of the *CpCdc13* on Ni-NTA agarose resin is described in Materials and Methods (7). Briefly, protein extract prepared as described above was incubated with Ni-NTA agarose resin for 1 hour at 4°C to promote binding of the tagged protein to Ni-NTA beads. Ni-NTA-protein extract mix was loaded onto a plastic 10 ml column by gravity and washed with five volumes of buffer E supplemented with 25 mM Imidazole. Imidazole solution disrupts protein-Ni-NTA binding. Use of low concentration of imidazole (below 100 mM) reduces non-specific protein-Ni-NTA binding, but only high imidazole concentration (300 mM and above) results in disruption of specific binding.

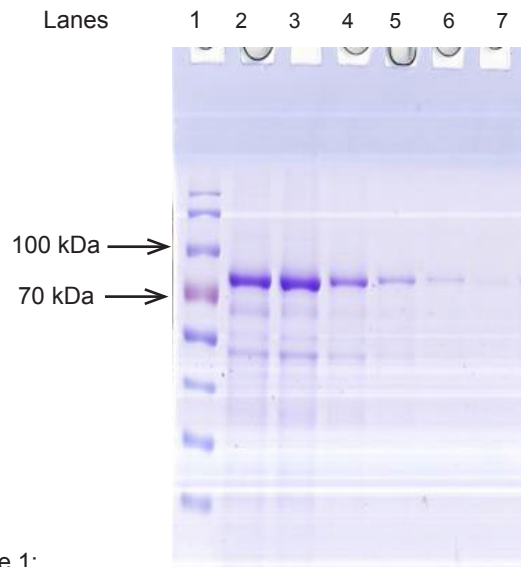


Figure 1: Elution of *CpCdc13* from Ni-NTA agarose column. Elution fraction were collected, and 3 $\mu$ l of protein solution from each fraction was resolved on denaturing polyacrylamide gel.

Lane1: Molecular weight marker  
 Lane 2: 300 mM Imidazole fraction 1  
 Lane 3: 300 mM Imidazole fraction 2  
 Lane 4: 300 mM Imidazole fraction 3  
 Lane 5: 300 mM Imidazole fraction 4  
 Lane 6: 300 mM Imidazole fraction 5  
 Lane 7: 300 mM Imidazole fraction 6

Protein was eluted with Buffer E supplemented with 300 mM Imidazole, and five 1.2 ml eluate fractions were collected. Protein concentration in eluate was determined using the Bradford method as described in Materials in Methods. Briefly, Bradford reagent (BioRad) was diluted five times with distilled water, and 1 ml of the solution was mixed with either a known amount of Bovine Serum Albumin (BSA) or protein samples collected at different steps of protein purification. Bradford reagent changes color upon addition of a protein solution, intensity of color change being depended on the amount of protein added. This change in color can be measured in spectrophotometer as an optical density of a solution (OD) at wavelength of 595 nm ( $OD_{595}$ ). Measuring  $OD_{595}$  of a known amount of protein in Bradford reagent solution allowed to determine a correlation between protein concentration and optical density of Bradford reagent-protein solution and construct a standard reference curve. This information was used to calculate protein concentration at the different steps of *Cdc13* purification. To assess the level of protein purification, protein solutions from different purification steps were also resolved by electrophoresis in polyacrylamide gel (Figure 1). Two fractions of eluate (2 and 3) were combined and frozen (6).



To remove histidine tag, protein samples from the previous step were subjected to digest with UPL1 protease (Figure 2). To separate digested protein, undigested protein and His-tag fragment, digestion reaction was loaded on Ni-NTA agarose. Flow through and elution with buffer E/50 mM imidazole was collected and analyzed by 10% SDS-PAGE (Figure 2) Proteins samples from lane were used to determine specificity of Cdc13 binding to telomeric DNA sequence.

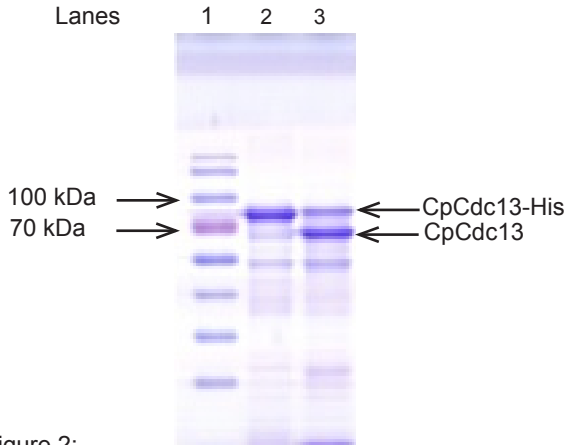


Figure 2:  
*CpCdc13-His-SUMO* digest with UPL1 protease.  
 His-tag was removed from Cdc13p protein by digesting it with UPL1 protease for 3 hours on ice as described in Materials and Methods. Samples of undigested and digested protein were resolved by electrophoresis in 10% SDS-PAGE

Lane1: Molecular weight marker  
 Lane 2: *CpCdc13-His-SUMO*  
 Lane 3: *CpCdc13-His-SUMO* digested with UPL1 protease

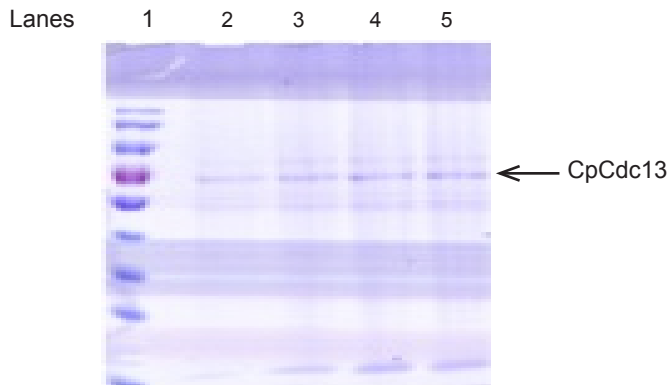


Figure 3:  
 Purification of *CpCdc13* on Ni-NTA agarose column.  
*CpCdc13* digested with UPL1 was loaded on Ni-NTA agarose column and binding reaction was allowed to proceed for 1 hour at 4°C. Flow through (unbound *CpCdc13* protein without the tag) was collected in 0.6 ml fractions. 10 µl sample of each fraction was loaded on 10% denaturing polyacrylamide gel

Lane1: Molecular weight marker  
 Lanes 2-5 Flow-through fractions 1-4.

**Gel shift mobility assay.**

The gel mobility assay is usually employed to assess the specificity of the DNA-protein binding. A protein is mixed with a radioactively labeled DNA fragment and the DNA-protein complex is formed. Products of the reaction are resolved in native polyacrylamide gel, where mobility of a chemical or a complex of chemicals depends on the size and charge of the chemical or its complex. The larger a chemical or the complex of several chemicals, the slower it migrates in a gel. Therefore, if a protein binds to DNA and the DNA-protein complex is formed, mobility of this DNA-protein complex will be lower as compared to mobility of the DNA fragment alone. It is said that the formation of a DNA-protein complex “shifts” the mobility of the DNA. If the binding is specific, than the amount of the radioactively labeled DNA-protein complex should increase when more protein is added to the reaction, and decrease with the addition of the identical but unlabeled DNA fragment.

*CpCdc13* protein was mixed with radioactively labeled and unlabeled single stranded DNA representing two copies of *C. parapsilosis* or *C. lusitania* telomeric repeat unit as described in Materials and Methods. Reactions were allowed to proceed for 20 minutes at room temperature, and the reaction mixes were resolved by electrophoresis in the native polyacrylamide gel. After completion of electrophoresis, gels were dried and exposed at a Phosphor screen. Image was obtained by scanning the Phosphor screen impressions (Figure 4).

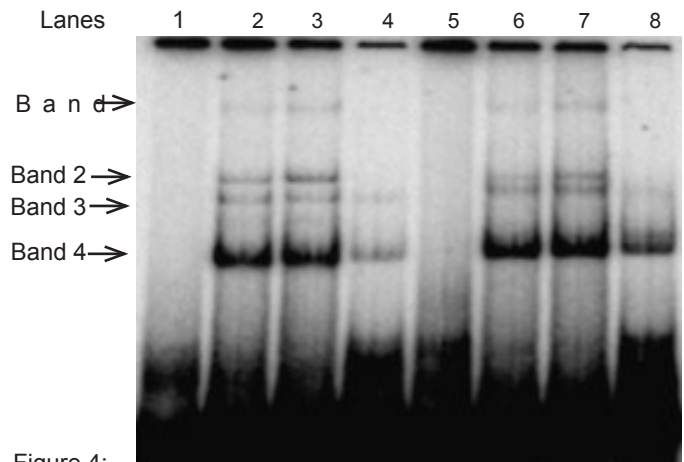


Figure 4:  
 Gel-shift assay. *CpCdc13* protein was mixed with radioactively labeled and unlabeled *Cpar* or *Clus* telomeric repeats (TEL). Reactions were allowed to proceed for 20 minutes and products were resolved by electrophoresis in the native polyacrylamide gel.

Lane1: *Cpar*TEL, no *CpCdc13* protein  
 Lane 2: *Cpar*TEL, 1 µl of *CpCdc13p* added  
 Lane 3: *Cpar*TEL 2 µl of *CpCdc13p* added  
 Lane 4: *Cpar*TEL, 2 µl of *CpCdc13p*, excess of cold *Cpar*TEL  
 Lane 5: *Clus*TEL, no *CpCdc13* protein  
 Lane 6: *Clus*TEL, 1 µl of *CpCdc13p* added  
 Lane 7: *Clus*TEL 2 µl of *CpCdc13p* added  
 Lane 8: *Clus*TEL, 2 µl of *CpCdc13p*, excess of cold *Clus*TEL

Intensity of signal of each band (Figure 4) was analyzed using ImageQuant software by Molecular dynamics (Figure 5).

Lanes 1 - 4 represent binding of *CpCdc13* to *C. parapsilosis* telomeric (*CparTEL*) DNA and lanes 5-8 represent binding of *CpCdc13* to *C. lusitaniae* telomeric DNA (*ClusTEL*). As seen on the gel image (Figure 4) and in the graph representation of radioactive signal intensity (Figure 5), only bands 1 and 2 signals were significantly reduced after addition of the excess of cold telomeric DNA (lanes 4 and 8). Therefore, only these two bands were considered to represent a specific *CpCdc13*/telomere binding complex. Additionally, binding of *CpCdc13* to *CparTEL* (lanes 2 and 3) and binding of *CpCdc13* to *ClusTEL* (lanes 6 and 7) were proportional to the amount of the protein input into the reaction (Figure 5). These data indicated that binding of *CpCdc13* to *CparTEL* and *ClusTEL* was specific.

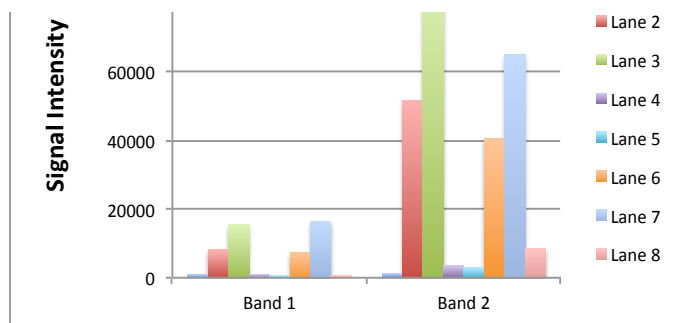


Figure 5: Gel-shift assay calculations. Results of the gel-shift assay were analyzed using the ImageQuant software. Each column corresponds to the lane on the gel. Intensity of the signal of the Band 1 complexes (lanes 1-8) and Band 2 complexes are presented separately as indicated on the graph. Composition of the reagents in reactions loaded in each lane is listed below.

Lane 1: *CparTEL*, no *CpCdc13* protein  
 Lane 2: *CparTEL*, 1  $\mu$ l of *CpCdc13p* added  
 Lane 3: *CparTEL* 2  $\mu$ l of *CpCdc13p* added  
 Lane 4: *CparTEL*, 2  $\mu$ l of *CpCdc13p*, excess of unlabeled *CparTEL*  
 Lane 5: *ClusTEL*, no *CpCdc13* protein  
 Lane 6: *ClusTEL*, 1  $\mu$ l of *CpCdc13p* added  
 Lane 7: *ClusTEL* 2  $\mu$ l of *CpCdc13p* added

## Discussion.

Orthologues of the *Cdc13* protein thought to be present in *Saccharomyces cerevisiae* only has now been discovered in various eukaryotic species. These proteins were ascribed to the *Cdc13*-like protein family on the basis of similarities between their telomere-related functions and that of the *ScCdc13*. However, the mechanism by which newly discovered *Cdc13* proteins interact with their respective telomeric DNA sequences is a subject of the debate. In one study, the interaction of *Candida Cdc13p* with their respective *Candida* telomeric sequences was found to be non-specific. In another study, *Cdc13* from *Candida* species were shown to bind the cognate telomere repeat specifically, and the affinity of *Cdc13*-DNA binding was enhanced by *Cdc13* dimer formation.

In this work we investigated the binding of *C. parapsilosis Cdc13* to telomeric sequences of *C. parapsilosis* and *C. lusitaniae*. Data demonstrated that *CpCdc13* was capable of binding to both *C. parapsilosis* and *C. lusitaniae* telomeric DNA while exhibiting higher affinity to *Clus* telomeric DNA sequence as compared to that of *Cpar TEL*. It is logical to conclude that *Candida Cdc13* proteins binding to telomeres is not highly specific. However, certain degree of similarity between *CparTEL* and *ClusTEL* and use of the truncated protein in this study may have affected overall results. Further experimental work is necessary to provide a more tangent evidence of specificity of *Candida Cdc13* proteins and elucidate the possible physiological explanation of this phenomenon.

## Acknowledgement

The author would like to thank Dr. Neal Lue for the opportunity to intern in his laboratory and Dr. Olga Steinberg Neifach for guidance and support.

This material is based upon work supported by the National Science Foundation under Grant No. MCB-1157305 to N.F. Lue and O. Steinberg Neifach

## References

1. Blackburn, E.H. (1991) Telomeres. Trends in Biochemical Sciences, 10:378-381.
2. Evans, S. K., and V. Lundblad. 1999. Est1 and Cdc13 as co-mediators of telomerase access. Science, 286:117–1203.
3. Garvik, B., M. Carson, and L. Hartwell. (1995) Single-stranded DNA arising at telomeres in cdc13 mutants may constitute a specific signal for the RAD9 checkpoint. Molecular and Cellular Biology, 15:6128-6138
4. Greider C.W. 1991 Telomeres. Current Opinions in Cell Biology, 3:444-451
5. Mandell EK, Gelinas AD, Wuttke DS, Lundblad V. 2011. Sequence- specific binding to telomeric DNA is not a conserved property of the Cdc13 DNA binding domain. Biochemistry, 50:6289 – 6291
6. Martin, V., Du, L.L, Rozenzhak, S., and P. Russell. 2007. Protection of telomeres by a conservative Stn1-Ten1 com-plex. Proceedings of the National Academy of Science of the United States of America, 104:14038-14043.
7. Rosario Ana. 2013. Cloning and Expression of CDC13 gene from Candida parapsilosis. Hostos Journal of Student Research, 4: 7-13
8. Surovtseva, Y.V., Churikov, D., Boltz, K.A., Song, X., Lamb, J.C., Warrington, R., Leehy, K., Heacock, M., Price, C., and D.E. Shippen. 2009 Conserved telomere maintenance component 1 interacts with STN1 and maintains chromosome ends in higher eukaryotes Molecular Cell, 36:207-2018
9. Yu, E.Y, Sun, J., Lei, M, and N. F. Lue . 2011. Analyses of Candida Cdc13 Orthologues Revealed a Novel OB Fold Dimer Arrangement, Dimerization-Assisted DNA Binding, and Substantial Structural Differences between Cdc13 and RPA70. Molecular and Cellular Biology, 32:186-198



Ms. Perez analyses experimental data obtained during her internship at the Weill Cornell Medical College.

---

Dear Reader,

Welcome to the third issue of the *Hostos Journal of Student Research* (HJSR)

The following are manuscript guidelines:

Scientific paper (definition).

Scientific paper has to be an original work by a student(s) composed under the mentorship of a faculty member of the Hostos Natural Sciences Department. A mentor's responsibility is to verify data and facts presented in the manuscript, and to avoid possible plagiarism by verifying citation references. Authorship of the paper should reflect the individual contributions of a student/students participating in the implementation of the research project. A mentor has to be included as one of the manuscript's authors.

Scientific essay/literature review (definition).

Scientific essay/literature review has to be an original work by a student submitted to a faculty member of the Hostos Natural Sciences Department. It is the faculty member's responsibility to verify facts presented in the essay, to make sure all conclusions of the essay are supported by scientific data, and to avoid possible plagiarism by verifying citation references. The name of the faculty member who helped the student with writing and editing the manuscript should appear next the student's name.

For example:

*Battle with the beasties: are they winning?*

John Smith and Olga Steinberg

Submissions

All submissions are to be made via e-mail. Requests for publication should come from the student in the form of a cover letter e-mailed to any member of the editorial board with the scientific manuscript attached in MS Word format. **Figures and charts in JPEG format with legends in MS Word format should be sent as separate files.** Contact information for both the student and the mentor should be included in the manuscript. Scientific papers and essays previously published/copyrighted elsewhere will not be accepted for publication in the *Hostos Journal of Student Research*.

All manuscript should have an abstract. Abstract is a short summary (less than 200 words) of ideas and conclusions included in the scientific paper.

All references have to conform to the APA standard.

### Sample submission letter:

Dear Editorial Board of the *Hostos Journal of Student Research*,

I would like to submit my manuscript (essay) titled....., authors.....  
for publication in the Natural Sciences Department on-line journal *Hostos Journal of Student Research*.  
All questions considering the context of the manuscript (essay) should be addressed to me. My contact information.....

Thank you for your consideration,

Name.....

---

Sample submission letter:

Dear Editorial Board of the *Hostos Journal of Student Research*,

I would like to submit my manuscript (essay) titled....., authors.....  
for publication in the Natural Sciences Department on-line journal *Hostos Journal of Student Research*.  
All questions considering the context of the manuscript (essay) should be addressed to me. My contact information.....

Thank you for your consideration,  
Name.....

### **Internship opportunities**

Summer internship at the Weill Cornell Medical College, Telomere laboratory of Dr. N.F. Lue  
Eligibility: students in AS, Forensic Science, and Engineering Programs recommended by their instructors.  
For more information, contact Professor Olga Steinberg at [osteinberg@hostos.cuny.edu](mailto:osteinberg@hostos.cuny.edu)

Summer internship at the City College, CUNY.  
Eligibility: students in Science programs who are registered to attend City College in the upcoming Fall semester.  
For more information, contact Professor Francisco Fernandez at [ffernandez@hostos.cuny.edu](mailto:ffernandez@hostos.cuny.edu)

Internship and PRISM Research opportunities at John Jay College, CUNY  
Eligibility: students in Forensic Science program only.  
For more information contact Professor Olga Steinberg at [osteinberg@hostos.cuny.edu](mailto:osteinberg@hostos.cuny.edu) or Outreach Coordinator of PRISM program Ms. Frances Jimenez at [fjimenez@jjay.cuny.edu](mailto:fjimenez@jjay.cuny.edu)

Front page photograph

Morphology of M-Ras KO astrocytes. (A) Immunofluorescence analysis of WT (\_\_\_) and M-Ras KO (\_\_\_) astrocytes. Astrocytes are stained with a Cy3-conjugated anti-GFAP antibody (red), and the actin cytoskeleton at the cell periphery was detected with an anti-phospho-ERM antibody (green). Two representative astrocytes are shown for each genotype. Magnification, X60.  
Courtesy of Nelson Nunez-Rodriguez

Nuñez Rodriguez N., Lee I.N., Banno A., Qiao H.F., Qiao R.F., Yao Z., Hoang T., Kimmelman A.C., and A.M. Chan. 2006  
*Mol Cell Biol.* 26:7145-54.

### **Hostos Journal of Student Research is a publication of the Natural Science Department, Hostos Community College, CUNY**

Chair of the Natural Science Department: Professor Francisco Fernandez.

Editorial Board:

Olga Steinberg, PhD, Editor In Chief	E-mail: <a href="mailto:osteinberg@hostos.cuny.edu">osteinberg@hostos.cuny.edu</a>
Flor Henderson, Ph.D	Email: <a href="mailto:fhenderson@hostos.cuny.edu">fhenderson@hostos.cuny.edu</a>
Julie Trachman, Ph.D	E-mail: <a href="mailto:jtrachman@hostos.cuny.edu">jtrachman@hostos.cuny.edu</a>
Yoel Rodriguez, PhD,	E-mail: <a href="mailto:yrodriguez@hostos.cuny.edu">yrodriguez@hostos.cuny.edu</a>